

REPORT DOCUMENTATION PAGE			2		Form Approved OMB NO. 0704-0188	
<p>The public reporting burden for this collection of information is estimated to average 1 hour per response, including the time for reviewing instructions, searching existing data sources, gathering and maintaining the data needed, and completing and reviewing the collection of information. Send comments regarding this burden estimate or any other aspect of this collection of information, including suggestions for reducing this burden, to Washington Headquarters Services, Directorate for Information Operations and Reports, 1215 Jefferson Davis Highway, Suite 1204, Arlington VA, 22202-4302. Respondents should be aware that notwithstanding any other provision of law, no person shall be subject to any penalty for failing to comply with a collection of information if it does not display a currently valid OMB control number.</p> <p>PLEASE DO NOT RETURN YOUR FORM TO THE ABOVE ADDRESS.</p>						
1. REPORT DATE (DD-MM-YYYY)		2. REPORT TYPE		3. DATES COVERED (From - To)		
		New Reprint		-		
4. TITLE AND SUBTITLE Hybridization of Phenylthiolate- and Methylthiolate-Adatom Species at Low Coverage on the Au(111) Surface				5a. CONTRACT NUMBER		
				W911NF-13-1-0101		
				5b. GRANT NUMBER		
6. AUTHORS Petro Maksymovych, Dan C. Sorescu, Oleksandr Voznyy, John T. Yates				5c. PROGRAM ELEMENT NUMBER		
				611102		
				5d. PROJECT NUMBER		
				5e. TASK NUMBER		
				5f. WORK UNIT NUMBER		
7. PERFORMING ORGANIZATION NAMES AND ADDRESSES				8. PERFORMING ORGANIZATION REPORT NUMBER		
University of Virginia P. O. Box 400195 Charlottesville, VA 22904 -4195						
9. SPONSORING/MONITORING AGENCY NAME(S) AND ADDRESS (ES) U.S. Army Research Office P.O. Box 12211 Research Triangle Park, NC 27709-2211				10. SPONSOR/MONITOR'S ACRONYM(S) ARO		
				11. SPONSOR/MONITOR'S REPORT NUMBER(S) 62064-CH.5		
12. DISTRIBUTION AVAILABILITY STATEMENT Approved for public release; distribution is unlimited.						
13. SUPPLEMENTARY NOTES The views, opinions and/or findings contained in this report are those of the author(s) and should not be construed as an official Department of the Army position, policy or decision, unless so designated by other documentation.						
14. ABSTRACT Using scanning tunneling microscopy we observed reaction products of two chemisorbed thiolate species, methylthiolate and phenylthiolate, on the Au(111) surface. Despite the apparent stability, organometallic complexes of methyl- and phenylthiolate with the gold adatom (RS ₂ Au ⁺ SR ⁻ , with R as the hydrocarbon group)						
15. SUBJECT TERMS SELF-ASSEMBLED MONOLAYERS; ADSORPTION; DECANETHIOL; THIOLATE						
16. SECURITY CLASSIFICATION OF:			17. LIMITATION OF ABSTRACT	15. NUMBER OF PAGES	19a. NAME OF RESPONSIBLE PERSON	
a. REPORT	b. ABSTRACT	c. THIS PAGE			John Yates	
UU	UU	UU	UU		19b. TELEPHONE NUMBER	
					434-924-7514	

Report Title

Hybridization of Phenylthiolate- and Methylthiolate-Adatom Species at Low Coverage on the Au(111) Surface

ABSTRACT

Using scanning tunneling microscopy we observed reaction products of two chemisorbed thiolate species, methylthiolate and phenylthiolate, on the Au(111) surface. Despite the apparent stability, organometallic complexes of methyl- and phenylthiolate with the goldadatom ($\text{RS}^*\text{Au}^*\text{SR}$, with R as the hydrocarbon group) undergo a stoichiometric exchange reaction, forming hybridized $\text{CH}_3\text{S}^*\text{Au}^*\text{SPh}$ complexes. Complementary density functional theory calculations suggest that the reaction is most likely mediated by a monothiolate RS^*Au complex bonded to the gold surface, which forms a trithiolate $\text{RS}^*\text{Au}^*(\text{SR})^*\text{Au}^*\text{SR}$ complex as a key intermediate. This work therefore reveals the novel chemical reactivity of the low-coverage “striped” phase of alkanethiols on gold and strongly points to the involvement of monoadatom thiolate intermediates in this reaction. By extension, such intermediates may be involved in the self-assembly process itself, shedding new light on this long-standing problem.

REPORT DOCUMENTATION PAGE (SF298) (Continuation Sheet)

Continuation for Block 13

ARO Report Number 62064.5-CH
Hybridization of Phenylthiolate- and Methylthiolæ...

Block 13: Supplementary Note

© 2013 . Published in Journal of the American Chemical Society, Vol. Ed. 0 135, (13) (2013), ((13). DoD Components reserve a royalty-free, nonexclusive and irrevocable right to reproduce, publish, or otherwise use the work for Federal purposes, and to authroize others to do so (DODGARS §32.36). The views, opinions and/or findings contained in this report are those of the author(s) and should not be construed as an official Department of the Army position, policy or decision, unless so designated by other documentation.

Approved for public release; distribution is unlimited.

Hybridization of Phenylthiolate- and Methylthiolate-Adatom Species at Low Coverage on the Au(111) Surface

Petro Maksymovych,^{*,†} Dan C. Sorescu,[‡] Oleksandr Voznyy,[§] and John T. Yates, Jr.^{*,||}

[†]Center for Nanophase Materials Sciences, Oak Ridge National Laboratory, Oak Ridge, Tennessee 37831, United States

[‡]United States Department of Energy, National Energy Technology Laboratory, Pittsburgh, Pennsylvania 15236, United States

[§]Department of Electrical and Computer Engineering, University of Toronto, Toronto, ON, M5S 3G4, Canada

^{||}Department of Chemistry, University of Virginia, Charlottesville, Virginia 22904, United States

S Supporting Information

ABSTRACT: Using scanning tunneling microscopy we observed reaction products of two chemisorbed thiolate species, methylthiolate and phenylthiolate, on the Au(111) surface. Despite the apparent stability, organometallic complexes of methyl- and phenylthiolate with the gold-adatom (RS-Au-SR, with R as the hydrocarbon group) undergo a stoichiometric exchange reaction, forming hybridized CH₃S-Au-SPh complexes. Complementary density functional theory calculations suggest that the reaction is most likely mediated by a monothiolate RS-Au complex bonded to the gold surface, which forms a trithiolate RS-Au-(SR)-Au-SR complex as a key intermediate. This work therefore reveals the novel chemical reactivity of the low-coverage “striped” phase of alkanethiols on gold and strongly points to the involvement of mono-adatom thiolate intermediates in this reaction. By extension, such intermediates may be involved in the self-assembly process itself, shedding new light on this long-standing problem.

Self-assembly of thiol and disulfide molecules on the gold surface continues to be a topic of broad interest in light of the growing utility of the thiolate self-assembly in a number of research applications^{1–3} as well as the need to develop a more predictive framework for tailoring molecules on surfaces. The present understanding of alkanethiolate self-assembly has been summarized in a number of review articles.^{4–6} Although it is generally agreed that thiolate molecules bond to the gold surface via gold-adatoms,^{7–9} the exact structural model, the number of gold adatoms bonded to the thiolate species, the degree of disorder, and the involvement of surface vacancies are still a matter of debate. But perhaps the most puzzling question is the actual mechanism of the self-assembly, and specifically the reactions by which S–H and S–S bonds dissociate, the gold adatoms are incorporated, and the subsequent self-assembly occurs. Understanding these processes is critical to allow a deterministic prediction of the experimental procedures that can lead to a well-ordered self-assembled monolayer of organosulfur molecules, the topology of the self-assembled patterns, and practical applications of the chemical reactivity of SAMs.¹

It is widely accepted that the self-assembly of most alkanethiols proceeds through a low-coverage, well-ordered two-dimensional phase termed the striped phase.¹⁰ The building blocks of the striped phase are organometallic complexes produced between two thiolate species and a gold-adatom, RS-Au(ad)-RS, which is sometimes referred to as the “staple”.^{4,11} In the case of the shortest alkanethiolate (CH₃S), the binding energy of the CH₃S-Au-SCH₃ complex to the Au(111) surface is 167.2 kcal/mol (with respect to isolated Au and CH₃S species), which is almost twice as large as ~86 kcal/mol of two CH₃S fragments, bonded directly to the Au(111) surface in their most stable bridge-fcc configuration.¹² Furthermore, the S–Au-adatom bond imposes strict steric constraints on the S–C bond angle relative to the surface plane, and thus upon the topology of the monolayer itself.¹³ Although the evolution of the striped phase as a whole with increasing surface coverage of alkanethiols was determined a long time ago,^{14,15} so far there is a lack of experiments or calculations that have addressed the detailed mechanism by which the striped phase reacts or evolves within the Au-adatom-based picture.

Here we present a scanning tunneling microscopy (STM) study of the coassembly between methylthiolate and phenylthiolate on the Au(111) surface at low-coverage that directly confirms the ability of the RS-Au-SR complexes to undergo a substitution reaction, conceptually similar to substitution reactions of the three-dimensional phases.^{14,17} The accompanying density functional theory (DFT) calculations imply the involvement of the singly coordinated adatom complexes, RS-Au, in the substitution reaction.

All the experiments were carried out in the ultrahigh vacuum environment, at a background pressure of <5 × 10^{–10} Torr as described previously.¹³ Phenylthiol (PhSH) and dimethyldisulfide (CH₃SSCH₃) precursor molecules were deposited onto a clean Au(111) surface held at ~70 K. Dissociation of the parent molecules and subsequent self-assembly of their products were carried out by slowly heating the surface to 250–300 K for up to 10 min. The surface was subsequently cooled down to 5 K for imaging in STM.

As we discussed earlier,¹⁸ thermal dissociation of phenylthiol on Au(111) at 300 K produces organometallic complexes (PhS-Au-SPh) that are stoichiometrically identical to those of

Received: January 4, 2013

Published: March 7, 2013

alkanethiolates, Figure 1a. Each complex has either a cis- or trans-configuration of the phenyl groups relative to the S–Au–

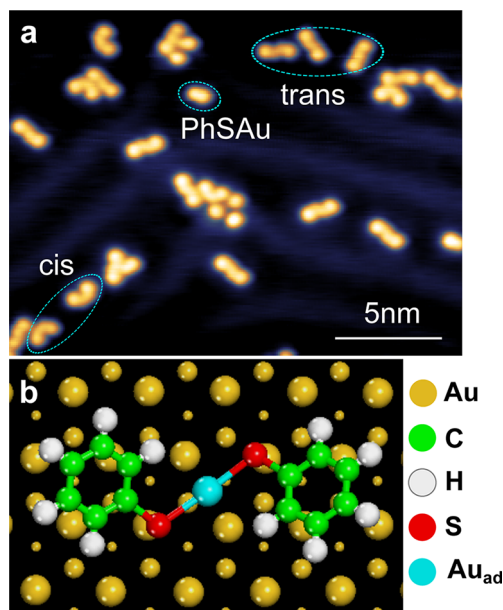


Figure 1. (a) STM image of PhS-Au-SPh complexes on the Au(111) surface. (b) Ball-model representation of the DFT-optimized structure of the trans-PhS-Au-SPh complex adsorbed on the Au(111) surface. Au_{ad} is the gold adatom.

S bond axis. To verify the orientation of the phenyl rings in these complexes, we have optimized their adsorbed structures by density functional theory calculations. The configuration shown in Figure 1b has a binding energy of 147.2 kcal/mol. The planes of both phenyl rings are tilted by 62°–65° relative to the surface normal, while the Au–S–C angles are 108.2°–110.1°. Therefore, the phenyl rings are clearly registered as two round shapes in the STM images (Figure 1a and ref 18). PhS-Au-SPh complexes do not self-assemble into the striped phase in its original definition because of the steric repulsion between the phenyl groups. However, the complexes do coalesce due to hydrogen bonding between aromatic hydrogen atoms and the sulfur headgroups.¹⁸

To induce the hybridization reaction between phenyl- and methylthiolate, dimethyldisulfide was deposited onto the gold surface with a preformed low coverage of phenylthiolate complexes (as in Figure 1a) at 70 K. Subsequently, the gold crystal was heated up to 300 K and cooled back to 5 K for STM imaging. Upon careful inspection of the STM images acquired after these procedures (Figure 2), three kinds of reaction products could be identified on the gold surface: (a) ordered 1D methylthiolate/Au stripes (e.g., ms in Figure 2a); (b) intact trans and cis PhS-Au-SPh complexes (pt and pc, respectively, in Figure 2a); (c) new hybrid reaction products (e.g., th, ch, respectively, in Figure 2a), which can be readily identified as an adatom complex PhS-Au-SCH₃. The identification is based on the discernible round shape of one phenyl ring on one side of the complex (Figure 2b white circle), a central feature corresponding to the adatom in the middle, and a methyl group on the other side of the complex (Figure 2b red circle). Moreover, the long axis of the complex is oriented almost normal to the $\langle 1\bar{1}0 \rangle$ direction of the gold surface, very similar to the orientation of the 1D stripes of methylthiolate. The

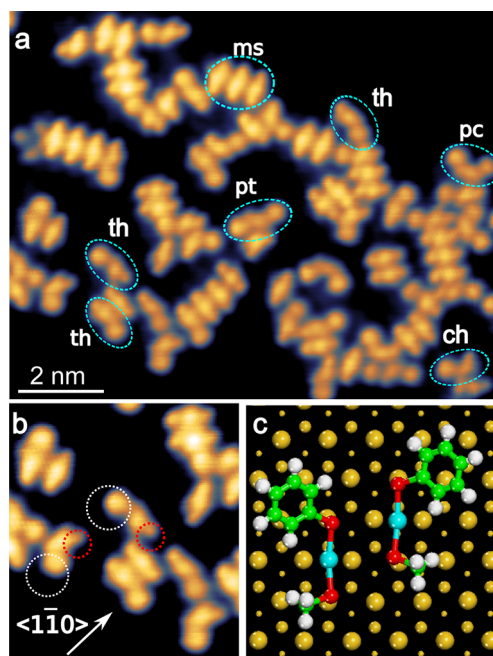
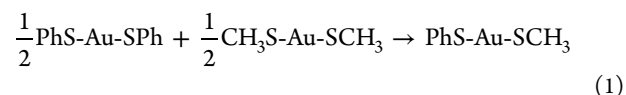


Figure 2. (a) STM image of the reaction products of the adsorption of CH₃SSCH₃ molecules onto a gold surface with a small coverage of PhS-Au-SPh complexes (Figure 1a). The labeled complexes are: ms-CH₃S-Au-SCH₃ stripe; pc(pt)-PhS-Au-SPh cis(trans) complexes; th(ch)-hybrid PhS-Au-SCH₃ trans(cis) complex formed upon the exchange reaction. (b) A close-up image of the area in (a) with several hybrid complexes. White (red) outlines mark the phenyl (methyl) groups, respectively. (c) A DFT-optimized structural model of cis-PhS-Au-SCH₃ complexes.

reaction between methyl- and phenylthiolate can therefore be represented as



Methyl and phenyl groups can be arranged in both cis (ch) and trans (th) relative positions around the S–Au–S bond axis in the hybrid complex (Figure 2a,b), with the majority of the complexes being trans. DFT calculations indicate a trans–cis isomerization barrier of about 11.5 kcal/mol (Supporting Figure S1), comparable to that of the methylthiolate complexes.^{13,19} Although we only acquired a limited set of STM images, we can verify that the substitution reaction was the only chemical transformation of the original phenylthiolate complexes, ruling out the desorption and decomposition reactions. The density of the phenyl groups before the hybridization reaction was measured to be 0.19 and 0.24 groups/nm² from two separate large-scale STM images, while following the reaction the density was 0.14 and 0.23 groups/nm². The scatter in numbers originated from the nonuniformity of the surface coverage due to the herringbone reconstruction, where the molecular species preferentially adsorb within periodically alternating fcc-stacked regions on the surface.^{7,20}

The mere fact of hybridization unambiguously confirms that contrary to the intuitive notion of the “robustness” of the RS-Au-SR complex, it turns out to be reactive around 300 K and the S–Au(adatom) bond can be broken and reformed. Unfortunately, the STM images and the location of the complexes provide few clues for the mechanism of the respective reactions. The hybridized PhS-Au-SCH₃ complexes

can sometimes be found as isolated species, but most frequently they either pair with another $\text{CH}_3\text{S-Au-SCH}_3$ or decorate the end of a $\text{CH}_3\text{S-Au-SCH}_3$ stripe (Figure 2). This observation confirms the identity of the hybrid complex as another type of the organometallic complex. However, it does not hint as to how a hybridization reaction may occur, because aggregation with another complex could have easily happened after the hybrid had formed.

We have therefore turned to DFT calculations to identify the possible reaction pathways and evaluate the plausibility of these pathways based on the magnitude of the activation barriers involved. Our first model was the hybridization and adatom rearrangement between PhS-Au-SPh and $\text{CH}_3\text{S-Au-SCH}_3$ complexes, with the initial relative orientation and spacing of the two complexes chosen to resemble that in the striped phase (Supporting Figure S2). Experimentally, we do observe a number of such “dimers” (see pt in Figure 2a for example). We have explored two reaction pathways: (1) a simultaneous exchange, where the S-Au-S bonds of the two complexes break and exchange with each other at the same time; (2) a sequential exchange, similar to (1), but separated in several consecutive steps (first, forming a trimer RS-Au-(RS)-Au-SR and a lone RS, followed by the reassociation into two RS-Au-SR dimers). For the reaction to occur in the temperature range between 250 and 300 K on the time scales of a typical annealing cycle (~ 10 min), the upper bound of the activation barrier height should be between 11 and 15 kcal/mol (estimated from the Arrhenius rate equation and a prefactor of 10^{13} s^{-1}).

The climbing-image nudged-elastic bands DFT calculation²¹ of the simultaneous exchange scenario between a PhS-Au-SPh and $\text{CH}_3\text{S-Au-SCH}_3$ pair revealed a prohibitively large activation barrier of ~ 33 kcal/mol (see Supporting Figure S2). A consecutive scenario lowers this barrier, but only a range of 19.4–20.1 kcal/mol depending on which molecule in the pair complex is dissociated first as seen in Supporting Figure S3. The lowest barrier calculated for the hybridization between PhS-Au-SPh and $\text{CH}_3\text{S-Au-SCH}_3$ complexes was 19.1 kcal/mol (see Figure S4). For reference, the reaction between two methylthiolate complexes, wherein two *trans*- $\text{CH}_3\text{S-Au-SCH}_3$ complexes become two *cis*- $\text{CH}_3\text{S-Au-SCH}_3$ complexes, has a barrier of 19.4 kcal/mol (see Figure S3). Altogether such values for the activation barrier are expected to be too large for the relevant temperature range based on the aforementioned estimate.

While it may be anticipated that the reason for the relatively high activation barriers in both cases (see Figures S3 and S4) is the large energy of the S-Au adatom bond, a closer inspection of the NEB trajectories reveals that the highest points actually correspond to the configuration where the RS-Au adatom entity (Figure S4 and Figure S5) is displaced from its 2-fold bridge site to approximately an atop site on the $\text{Au}(111)$ surface. Thus the energy peaks when CH_3S begins to displace away from the parent complex, *after* the S-Au(ad) bond has been broken. A straightforward inspection of the lattice spacings and of the allowed adsorption sites available for the reaction leads to the conclusion that this unfavorable geometry cannot be avoided if one wants to maintain a closely spaced transition-state complex of two dissociating/hybridizing RS-Au-SR complexes.

We therefore explored an alternative route to hybridization, where $\text{CH}_3\text{S-Au}$ (or PhS-Au) species, rather than the $\text{CH}_3\text{S-Au-SCH}_3$ complex, participate in the hybridization reaction (Figure 3). Reaction 1 is then split in at least two steps, for example:

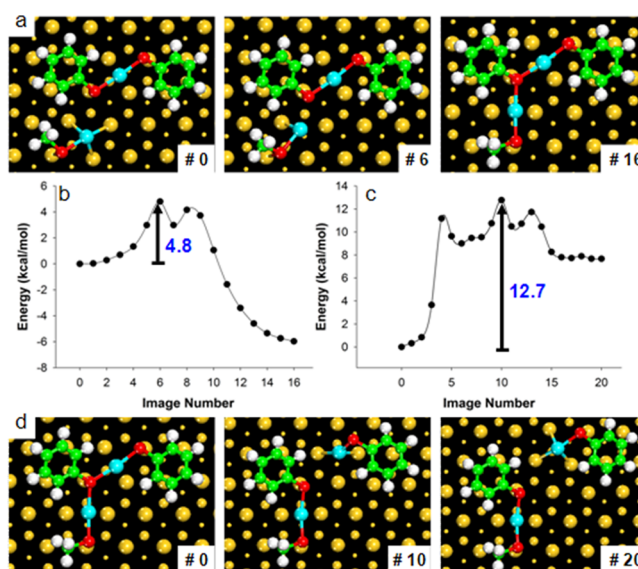
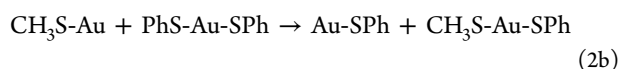
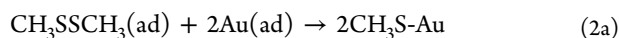


Figure 3. Minimum energy pathways for (a,b) reaction of $\text{CH}_3\text{S-Au}$ with PhS-Au-SPh with the formation of $\text{CH}_3\text{S-Au-(SPh)-Au-SPh}$ intermediate complex followed by (c,d) separation reaction of the PhS-Au fragment with formation of $\text{CH}_3\text{S-Au-SPh}$. For each reaction the atomic configurations in the initial, several transition, and final states are indicated.

The $\text{CH}_3\text{S-Au}$ or PhS-Au species as reactants in the hybridization reaction can overcome the energetically prohibitive intermediate states, by allowing $\text{CH}_3\text{S-Au}$ to approach the PhS-Au-SPh complex (or PhS-Au to approach the $\text{CH}_3\text{S-Au-SCH}_3$ complex) through a series of diffusion steps, each of which has a barrier < 5 kcal/mol (with similar values for both $\text{CH}_3\text{S-Au}$ and PhS-Au , and consistent with calculations by Cometto et al.²²). For $\text{CH}_3\text{S-Au}$ we considered both lying down and vertical initial configurations prior to hybridization, as shown in Figure 3 and in Supporting Information (Figure S5a). Once in a favorable position, the two reactants form an intermediate tricentric organometallic complex, $\text{CH}_3\text{S-Au-(SPh)-Au-SPh}$ (Figure 3a), which is surprisingly stable thermodynamically. The lowest barrier calculated for this process is only ~ 4.8 kcal/mol (Figure 3b), while the net energy gain is 6 kcal/mol relative to PhS-Au-SPh and $\text{CH}_3\text{S-Au}$ bonded in their preferred configurations on the $\text{Au}(111)$. Subsequent separation of the Au-SPh fragment now proceeds through a maximum barrier of ~ 12.7 kcal/mol (Figure 3c,d), which is feasible for the temperature range of our experiments. Thus, invoking RSAu species in the hybridization reaction reduces the maximum activation barrier height by as much as ~ 15 kcal/mol, relative to the simultaneous exchange mechanism between a PhS-Au-SPh and a $\text{CH}_3\text{S-Au-SCH}_3$ pair. In the case when a PhS-Au group reacts with a $\text{CH}_3\text{S-Au-SCH}_3$ molecule the corresponding diffusion and hybridization barriers are also relatively small with values less than 6.2 kcal/mol (see Figure S5b). Therefore, both scenarios for hybridization, including either reaction of $\text{CH}_3\text{S-Au}$ with PhS-Au-SPh or reaction of PhS-Au with $\text{CH}_3\text{S-Au-SCH}_3$ are kinetically feasible.

The existence of the RS-Au adatom complexes on the surface requires justification. At present the reaction pathway from an adsorbed thiol RSH or dimethyldisulfide RSSR molecule to the organometallic complexes is not fully understood.^{4–6} But the mere fact that chemisorption of thiol RSH molecules yields the same type of adatom complexes as RSSR⁸ suggests that the RS-Au species must form and exist on the surface at some point in the temperature range corresponding to the self-assembly reaction. Also, in the case of phenylthiolate, we do observe features that could be assigned to PhS-Au (Figure 1a). At the same time, earlier theoretical models and several experiments have implicated RS-Au species as the actual building blocks of the SAMs.^{7,23,24} Cometto et al. suggested that RS-Au species may be the favorable intermediate in the self-assembly process based on the lower diffusion barrier compared to both RS and the gold adatom itself over the gold surface.²² Moreover, a model for the $\sqrt{3} \times \sqrt{3} R30^\circ$ phase of the methylthiolate on gold at 300 K proposed by Mazzarello et al.²³ involves a dynamic equilibrium between the $\text{CH}_3\text{S-Au-SCH}_3$ complexes and bridge-bonded $\text{CH}_3\text{S-Au}$ species supported by the DFT-MD calculations. From our own DFT-NEB calculations, the barrier height to break a single S-Au-S headgroup, forming a $\text{CH}_3\text{S-Au}$ species and a bridge-fcc bonded CH_3S fragment was calculated to be ~ 16.6 kcal/mol (Figure S6a). The barrier to break PhS-Au-SPh and form PhS-Au species is only 15.9 kcal/mol (Figure S6b). Both values are on the borderline of thermally allowed reactions around 300 K, and we therefore cannot exclude the possibility of a nonzero equilibrium surface coverage of $\text{CH}_3\text{S-Au}$ or PhS-Au coexisting with, respectively, $\text{CH}_3\text{SAuSCH}_3$ and PhS-Au-SPh during the hybridization reaction. In addition, the involvement of defect sites such as atomic steps or dislocation sites on the herringbone reconstruction may play a role in reducing the activation energy for these individual bond breaking steps.

To summarize, we have directly observed a first example of hybridization reaction between alkyl- and phenylthiolate species, bonded to the surface in the form of organometallic complexes with gold adatoms. Using density functional theory, we have evaluated a series of possible reaction pathways that lead to hybridization and concluded that a direct reaction between two organometallic complexes is unlikely. However, involving singly coordinated $\text{CH}_3\text{S-Au}$ complexes does allow for an exchange reaction with the PhS-Au-SPh complexes through a tricentric intermediate, with a maximum barrier height of ~ 12.7 kcal/mol. More generally, our observations emphasize that the striped phase by itself is reactive at around 300 K, and S–Au–S bonds can be broken. The evolution toward the high coverage 3D ordered phase through a series of striped phases must consider the possibility of such ligand exchange reactions as well as the likely involvement of RS-Au intermediates in the process.

■ ASSOCIATED CONTENT

Supporting Information

Supplementary DFT calculations. This material is available free of charge via the Internet at <http://pubs.acs.org>.

■ AUTHOR INFORMATION

Corresponding Author

maksymovychp@ornl.gov; jty2n@virginia.edu

Notes

The authors declare no competing financial interests.

■ ACKNOWLEDGMENTS

P.M. and J.T.Y. acknowledge the W. M. Keck Foundation grant to the W. M. Keck Center for Molecular Electronics at the University of Pittsburgh, ARO and NEDO (Japan) for financial support. P.M.: Research performed in part at the Center for Nanophase Materials Sciences, Oak Ridge National Laboratory, Division of User Facilities, U.S. Department of Energy. We acknowledge a grant of computer time at the Pittsburgh Supercomputer Center.

■ REFERENCES

- (1) Love, J. C.; Estroff, L. A.; Kriebel, J. K.; Nuzzo, R. G.; Whitesides, G. M. *Chem. Rev.* **2005**, *105*, 1103–1169.
- (2) Lazznerini, G. M.; Mian, S.; Di Stasio, F.; Merari Masillamani, A.; Crivillers, N.; Reinders, F.; Mayor, M.; Samori, P.; Cacialli, F. *Appl. Phys. Lett.* **2012**, *101*, 153306.
- (3) Gundlach, D. J.; Royer, J. E.; Park, S. K.; Subramanian, S.; Jurchescu, O. D.; Hamadani, B. H.; Moad, A. J.; Kline, R. J.; Teague, L. C.; Kirillov, O.; Richter, C. A.; Kushmerick, J. G.; Richter, L. J.; Parkin, S. R.; Jackson, T. N.; Anthony, J. E. *Nat. Mater.* **2008**, *7*, 216–221.
- (4) Hakkinen, H. *Nat. Chem.* **2012**, *4*, 443.
- (5) Maksymovych, P.; Voznyy, O.; Dougherty, D. B.; Sorescu, D. C.; Yates, J. T., Jr. *Prog. Surf. Sci.* **2010**, *85*, 206–240.
- (6) Vericat, C.; Vela, M. E.; Benitez, G.; Carro, P.; Salvarezza, R. C. *Chem. Soc. Rev.* **2010**, *39*, 1805–34.
- (7) Yu, M.; Bovet, N.; Satterley, C. J.; Bengio, S.; Lovelock, K. R. J.; Milligan, P. K.; Jones, R. G.; Woodruff, D. P.; Dhanak, V. *Phys. Rev. Lett.* **2006**, *97*, 166102.
- (8) Maksymovych, P.; Sorescu, D. C.; Yates, J. T., Jr. *Phys. Rev. Lett.* **2006**, *97*, 146103.
- (9) Cossaro, A.; Mazzarello, R.; Rousseau, R.; Casalis, L.; Verdini, A.; Kohlmeier, A.; Floreano, L.; Scandolo, S.; Morgante, A.; Klein, M. L.; Scoles, G. *Science* **2008**, *321*, 943–946.
- (10) Poirier, G. E. *Chem. Rev.* **1997**, *97*, 1117–1128.
- (11) Jadzinsky, P. D.; Calero, G.; Ackerson, C. J.; Bushnell, D. A.; Kornberg, R. D. *Science* **2007**, *318*, 430–3.
- (12) Maksymovych, P.; Sorescu, D. C.; Yates, J. T., Jr. *J. Phys. Chem. B* **2006**, *110*, 21161–21167.
- (13) Voznyy, O.; Dubowski, J. J.; Yates, J. T.; Maksymovych, P. *J. Am. Chem. Soc.* **2009**, *131*, 12989–93.
- (14) Fitts, W. P.; White, J. M.; Poirier, G. E. *Langmuir* **2002**, *18*, 2096–2102.
- (15) Poirier, G. E. *Langmuir* **1999**, *15*, 1167–1175.
- (16) Xu, G.; Woodruff, D. P.; Bennett, N.; Elliott, M.; Macdonald, J. E. *Langmuir* **2010**, *26*, 8174–8179.
- (17) Dameron, A. A.; Charles, L. F.; Weiss, P. S. *J. Am. Chem. Soc.* **2005**, *127*, 8697–8704.
- (18) Maksymovych, P.; Yates, J. T., Jr. *J. Am. Chem. Soc.* **2008**, *130*, 7518–7519.
- (19) Jiang, D.-en; Dai, S. *Phys. Chem. Chem. Phys.* **2009**, *11*, 8601–5.
- (20) Fernandez-Torrente, I.; Monturet, S.; Franke, K. J.; Fraxedas, J.; Lorente, N.; Pascual, J. I. *Phys. Rev. Lett.* **2007**, *99*, 176103.
- (21) (a) Jónsson, H.; Mills, G.; Jacobsen, K. W. *Computer Simulation of Rare Events and Dynamics of Classical and Quantum Condensed-Phase Systems - Classical and Quantum Dynamics in Condensed Phase Simulations*; World Scientific: Singapore, 1998; p 385. (b) Henkelman, G.; Uberuaga, B. P.; Jónsson, H. *J. Chem. Phys.* **2000**, *113* (22), 9901.
- (22) Cometto, F. P.; Paredes-Olivera, P.; Macagno, V. A.; Patrito, E. M. *J. Phys. Chem. B* **2007**, *109*, 21737.
- (23) Mazzarello, R.; Cossaro, A.; Verdini, A.; Rousseau, R.; Casalis, L.; Danisman, M. F.; Floreano, L.; Scandolo, S.; Morgante, A.; Scoles, G. *Phys. Rev. Lett.* **2007**, *98*, 16102.
- (24) Di Felice, R.; Selloni, A. *J. Chem. Phys.* **2004**, *120*, 4906–14.